

ISTITUTO NAZIONALE DI FISICA NUCLEARE

Sezione di Trieste

Submitted to Applied Physics B

INFN/BE-93/02

9 marzo 1993

P. Micossi, F. Della Valle, E. Milotti, C. Rizzo, G. Ruoso and E. Zavattini

MEASUREMENT OF THE BIREFRINGENCE PROPERTIES OF THE REFLECTING SURFACE OF AN INTERFERENTIAL MIRROR

MEASUREMENT OF THE BIREFRINGENCE PROPERTIES OF THE REFLECTING SURFACE OF AN INTERFERENTIAL MIRROR

P. Micossi , F. Della Valle , E. Milotti and E. Zavattini

Dipartimento di Fisica dell'Università di Trieste, Italy
and
Istituto Nazionale di Fisica Nucleare, Sezione di Trieste, Italy

C. Rizzo

Istituto Nazionale di Fisica Nucleare, Sezione di Trieste,
Laboratori - Area di Ricerca, Trieste, Italy

G. Ruoso

Dipartimento di Fisica "Galileo Galilei" dell'Università di Padova, Italy
and
Istituto Nazionale di Fisica Nucleare, Laboratori Nazionali di Legnaro, Legnaro (PD), Italy

Abstract.

We have set up an apparatus to measure the ellipticity acquired by a linearly polarized light beam after a single quasi-normal reflection on an interferential mirror. Results of measurements performed on a standard 10 cm diameter interferential mirror are presented.

1. Introduction.

In the last few years some experiments have been performed to measure small ellipticities acquired by a linearly polarized laser beam propagating through a high magnetic field region both in vacuum and in gases [1]. In these experiments multipass optical cavities [2] obtained with interferential mirrors have been used to increase the length of the optical path in the magnetic field region. The use of high finesse Fabry-Perot cavities to measure the vacuum birefringence due to a high magnetic field [3] has been also recently proposed [4].

In all these experiments one of the sources of noise and systematic errors is the fact that reflecting on the surface of the interferential mirror the light beam acquires an ellipticity. Several experimental studies of the birefringence properties of interferential mirrors exist [5,6,7]. However, these studies either have been done with many reflections in a multipass cavity [5,6], covering therefore a rather large surface, and therefore the results give essentially average birefringence properties of the surface, or have been obtained with the light passing through the mirror substrate [7] which might contribute to the ellipticity.

The observed ellipticity [5,6] gained by the beam in the reflection is due to two effects. The first one is related to off-normal reflection and depends on incidence angle i . The second one, independent from i , suggests the presence of a non isotropic structure on the reflecting surface. This effect generally ranges between 10^{-3} and 10^{-5} .

We present here an apparatus devised to measure the birefringence introduced in a linearly polarized laser beam by a single reflection at a given point of the surface. The apparatus has been optimised to measure the part independent from the incidence angle i . We present results on the birefringence distribution over the reflecting surface of one of the mirrors for which the average birefringence over a large region has been measured in a multipass cavity and reported in ref 6.

2. Experimental apparatus.

A schematic drawing of the experimental apparatus is shown in fig. 1.

The light source is a 5 mW continuous wave He-Ne laser ($\lambda = 633$ nm). The light, linearly polarized by the prism P [model MGLADW12, Karl Lambrecht] enters the photoelastic modulator PEM [model PEM90 1/FS50, Hinds Instruments] which introduces in the beam a relatively large and controlled modulated ellipticity at frequency $f_M \approx 50$ KHz. The experimental set up is chosen so that the light polarization is in the incidence plane and the birefringence axes of the modulator are at 45° with respect to the light polarization itself. After reflection at the mirror point Q the beam is analysed by the prism A. The transmitted light, after being focused by the lens L (30 cm focal length), is detected by the preamplified photodiode PD [model S4754, Hamamatsu].

The mirror M was mounted on movement stages and the whole mechanical part is mounted on an optical table [model ART312SNMX, Aerotech] that can rotate with a frequency ν up to 0.5 Hz. The normal to the mirror M in the point Q to be analysed is always set coincident with the axis of rotation of the table. A synchronisation signal from the table triggers data acquisition performed by a spectrum analyser.

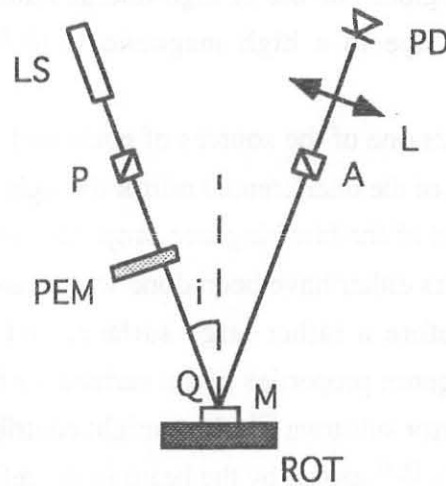


Fig. 1. Simplified sketch of the layout; LS : laser light source; P : Polarizer prism; PEM : photoelastic modulator; Q : reflection point, M : interferential mirror; ROT : rotating optical table; A : analyser prism; L : focusing lens, PD : photodiode, i : incidence angle (about 10°).

To check and monitor the stability of the reflected beam before every measurement we replaced the photodiode PD with the position sensitive photodiode S [model S1880, Hamamatsu]. The photodiode S has a sensitive area of $12 \times 12 \text{ mm}^2$, and it outputs two voltages proportional to the cartesian coordinates of the incidence point on the photodiode surface which are monitored by a 9 bit ADC.

The rotating table is set horizontal and all other mechanical and optical parts are put on a vertical structure 1 m high; the incidence angle i is about 10° .

3. Method and data analysis.

A Jones matrix representation [8] was used to derive the expected signal. The matrix

$$M = e^{\frac{i\delta}{2}} \begin{bmatrix} 1 + i\frac{\delta}{2} \cos 2\vartheta(t) & -i\frac{\delta}{2} \sin 2\vartheta(t) \\ -i\frac{\delta}{2} \sin 2\vartheta(t) & 1 - i\frac{\delta}{2} \cos 2\vartheta(t) \end{bmatrix}$$

represents the mirror, where δ is a small phase difference due to the mirror birefringence and $\vartheta(t)$ is the angle between the birefringence axis and the polarization direction of incident light. Because of table rotation $\vartheta(t) = 2\pi\nu t + \vartheta_0$. The photoelastic modulator is represented by:

$$\text{PEM} = e^{\frac{i\varphi(t)}{2}} \begin{bmatrix} \cos \frac{\varphi(t)}{2} & -i \sin \frac{\varphi(t)}{2} \\ -i \sin \frac{\varphi(t)}{2} & \cos \frac{\varphi(t)}{2} \end{bmatrix}$$

where $\varphi(t) = \varphi_0 \cos(2\pi f_M t + \Phi_M)$ is the time varying phase difference. During data taking we used $\nu = 234.375$ mHz, $\varphi_0 = 0.396$ and $f_M \approx 50$ kHz. The matrix

$$\text{UB} = e^{\frac{i\eta}{2}} \begin{bmatrix} 1 + \frac{i\eta}{2} \cos 2\chi & -\frac{i\eta}{2} \sin 2\chi \\ -\frac{i\eta}{2} \sin 2\chi & 1 - \frac{i\eta}{2} \cos 2\chi \end{bmatrix}$$

takes into account any uncompensated birefringence that does not vary with time or drifts very slowly over a table cycle such as the off-normal component of the ellipticity. In our case η was of the order of 10^{-2} . χ is the angle between the axis of the uncompensated birefringence and the light polarization. The matrix

$$\text{A} = \begin{bmatrix} 0 & 0 \\ 0 & 1 \end{bmatrix}$$

represents the analysing polarimeter.

The light power incident on the photodiode can be computed as :

$$\begin{aligned} W(t) &= W \left| \text{A M UB PEM} \begin{pmatrix} I \\ 0 \end{pmatrix} \right|^2 = \\ &= W \left\{ \sigma^2 + \sin^2 \frac{\varphi(t)}{2} + \frac{\eta}{2} \sin \varphi(t) \sin 2\chi + \frac{\delta}{2} \sin \varphi(t) \sin 2\vartheta(t) \right\} \end{aligned} \quad (1)$$

where W is the light power before the analysing prism A , typically $100 \mu\text{W}$; σ^2 is the extinction factor, typically of the order of 10^{-7} . The terms of order δ^2 , η^2 and $\eta\delta$ have been neglected. Using the integral representation of the Bessel function of integer order [9], we can expand eq. 1 as follows

$$W(t) = W \left\{ \sigma^2 + \frac{1 - J_0(\varphi_0)}{2} + \eta \sin 2\chi J_1(\varphi_0) \cos(2\pi f_M t + \Phi_M) + \right. \\ \left. + \delta J_1(\varphi_0) \cos(2\pi f_M t + \Phi_M) \sin(2\pi \nu t + \vartheta_0) + J_2(\varphi_0) \cos(4\pi f_M t + 2\Phi_M) \right\} \\ + \text{higher frequency terms} \quad (2)$$

where J_0 , J_1 and J_2 are Bessel functions of order, respectively, 0, 1 and 2. For $\varphi_0=0.396$ we have $J_0(\varphi_0)=0.961179$, $J_1(\varphi_0)=0.194144$ and $J_2(\varphi_0)=0.0193471$. In table 1 we show the main spectral components of the signal indicated by eq. (2).

Table 1
Main spectral components of the signal given by eq. 2

Component	frequency	amplitude	phase
W_{DC}	0	$W \{ \sigma^2 + (1/2)[1 - J_0(\varphi_0)] \}$	
W_-	$f_M - 2\nu$	$W \psi_0 J_1(\varphi_0)$	$\Phi_- = \Phi_M - 2\vartheta_0$
W_M	f_M	$W \eta J_1(\varphi_0)$	Φ_M
W_+	$f_M + 2\nu$	$W \psi_0 J_1(\varphi_0)$	$\Phi_+ = \Phi_M + 2\vartheta_0$
W_{2M}	$2f_M$	$W J_2(\varphi_0)$	$\Phi_{2M} = 2\Phi_M$

The amplitude of the ellipticity to be measured $\psi_0 = \delta/2$ is given by

$$\psi_0 = \frac{W_- J_2(\varphi_0)}{W_{2M} J_1(\varphi_0)} = \frac{W_+ J_2(\varphi_0)}{W_{2M} J_1(\varphi_0)} \quad (3)$$

and the direction of the birefringence axis ϑ_0 is

$$\vartheta_0 = \frac{\Phi_+ - \Phi_-}{4} \quad (4)$$

4. Results and discussion.

In fig. 2 we show the typical variation with time of the values of the coordinates of the light spot on the surface of the position sensitive photodiode S (modulator off and prism A set to maximum transmission) corresponding to a displacement of about 0.03 mm at the table rotation frequency ν . The noise of the photodiode itself corresponds to about 0.01 mm.

In the same conditions replacing photodiode S with photodiode PD, we found frequency spectra similar to the one shown in fig. 3 : the two first highest peaks, corresponding to W_v e W_{2v} , are clearly visible.

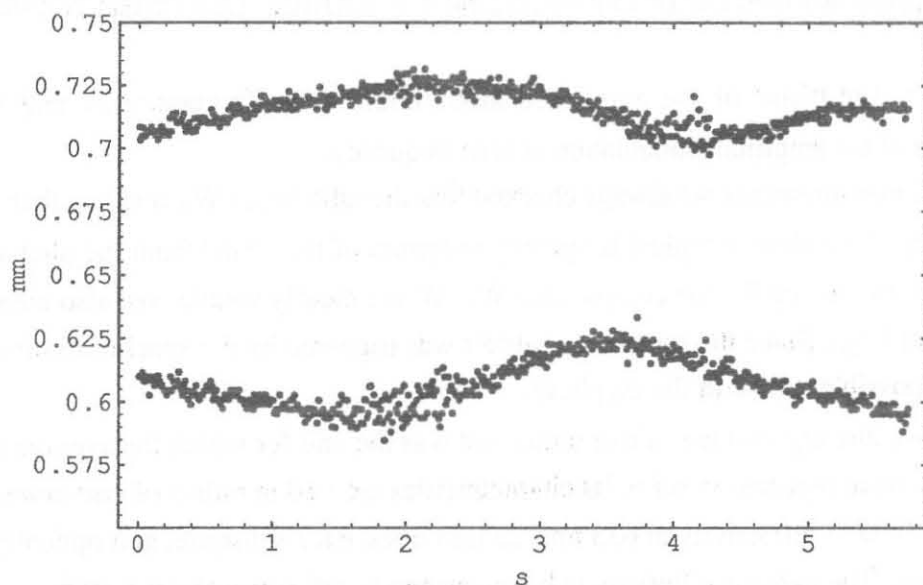


Fig. 2 : Coordinates of the laser light spot on the position sensitive photodiode S for pointing stability of about 0.03 mm (modulator off, prism A set to maximum transmission).

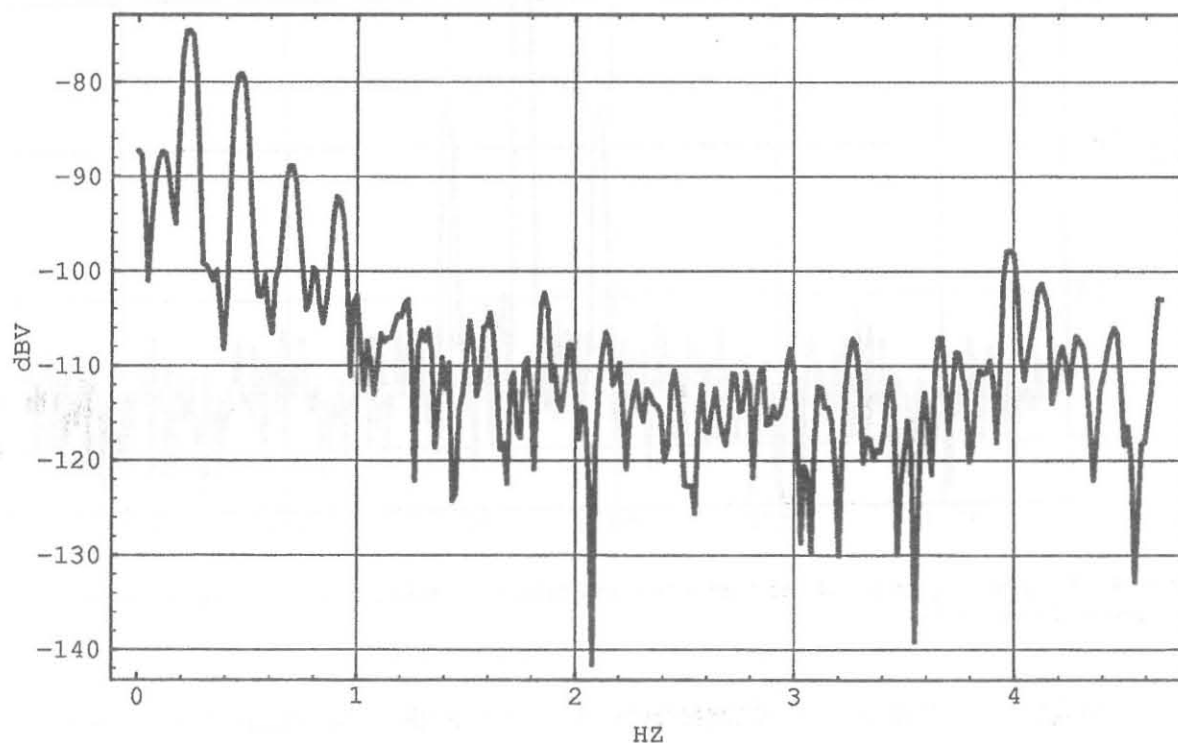


Fig.3 : Frequency spectrum of the total signal (modulator off, prism A set to maximum transmission) corresponding to a pointing stability of about 0.03 mm.

From eq. 2 one can derive the components at the $f_M \pm 2\nu$ frequency of the total signal (modulator on, prism A set at maximum extinction) due to an eventual spurious amplitude modulation

$$W_{\pm} = W_0 \psi_0 J_1(\varphi_0) \cos[2\pi(f_M \pm 2\nu)t + \Phi_M \pm 2\vartheta_0] + W_{2\nu} \eta J_1(\varphi_0) \cos[2\pi(f_M \pm 2\nu)t + \Phi_M \pm \rho] \quad (5)$$

where ρ is the phase of the amplitude modulation at the frequency 2ν and W_0 is the amplitude of the amplitude modulation at zero frequency.

During all measurements we always checked that the ratio $W_{2\nu}/W_0$ was less than $5 \cdot 10^{-4}$.

In fig. 4 we show a typical frequency spectrum of the signal from the photodiode PD around the frequency f_M ; the components W_+ , W_- are clearly visible. We also measured the component W_{2M} . Since the spectrum analyser was triggered by the synchronisation signal it was also possible to obtain the ϑ_0 phase.

As we already said the mirror under test was the one for which the average ellipticity properties were reported in ref 6. Its characteristics are : 10 m radius of curvature, 10.0 cm diameter, 0.9983 reflectivity at 633 nm, 22 mm thick BK7 substrate, and optically cleaned backsurface. The average ellipticity value measured in ref. 6 was about $5 \cdot 10^{-4}$.

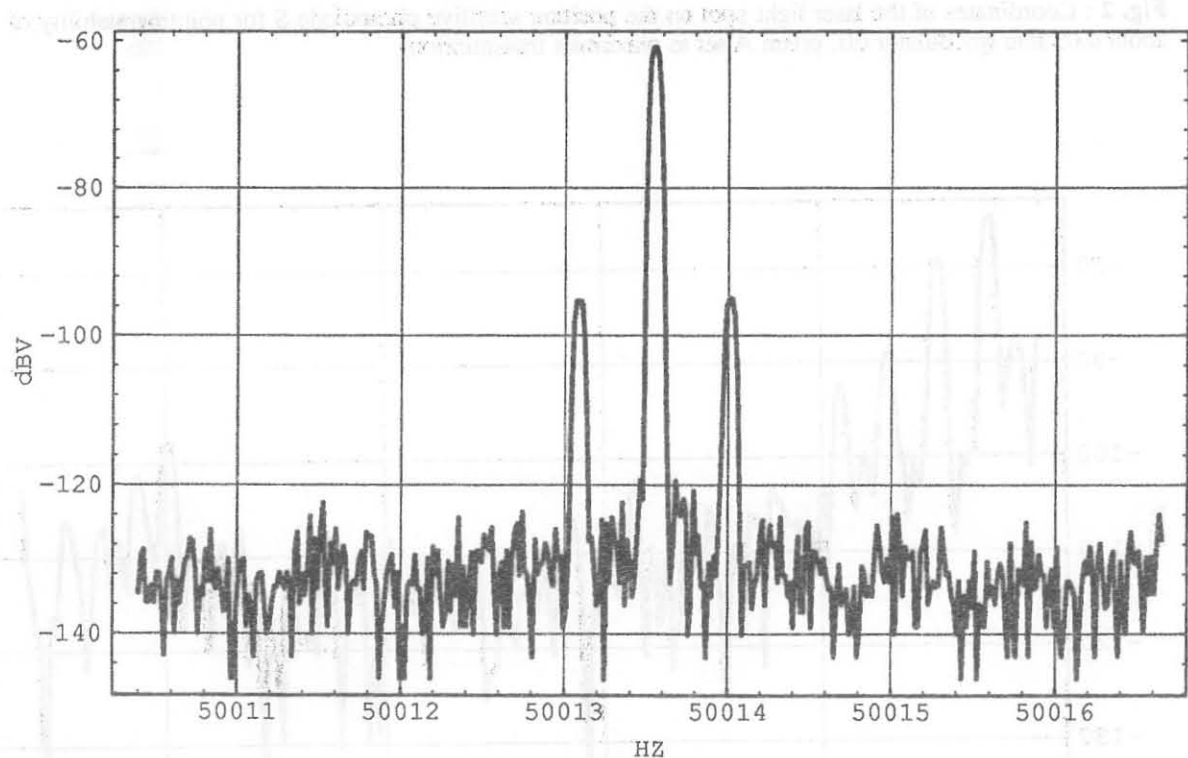


Fig. 4 : Frequency spectrum of the total signal (modulator on, prism A set at maximum extinction) around the frequency f_M .

In fig. 5 we show a pictorial representation of our results : the length of the arrows are proportional to the ellipticity measured while the direction of the birefringence axis is indicated by the direction of the arrow itself.

In table 2 we list the values of ψ_0 and ϑ_0 for each point together with the corresponding coordinates on the mirror surface. The values of ψ_0 range from $1.4 \cdot 10^{-4}$ to $3.1 \cdot 10^{-4}$, ϑ_0 ranges from -24° to 15° . These values are compatible with the value of the average ellipticity found in ref. 6.

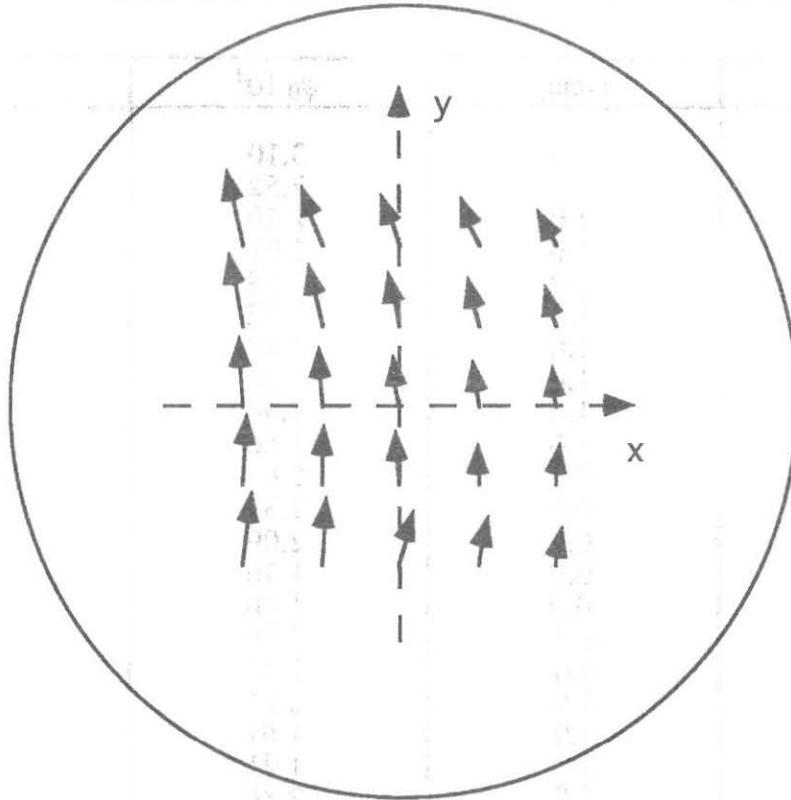


Fig. 5 : Pictorial representation of the birefringence properties of the mirror analysed. The length of the arrows are proportional to the ellipticity measured, the direction of the local birefringence axis is indicated by the direction of the arrow itself.

The error is mainly due to residual modulation in W : from eq. 5 one can derive that the maximum error on ψ_0 is given by

$$\Delta\psi_0 = \frac{W_{2\nu}\eta}{W_0} \quad (6)$$

while for ϑ_0 is

$$\Delta\vartheta_0 = \frac{W_{2\nu}\eta}{W_0\psi_0} \quad (7)$$

With our experimental parameters we have $\Delta\psi_0 < 5 \cdot 10^{-6}$ and $\Delta\vartheta_0 < 1^\circ$. The sensitivity of the apparatus was typically $10^{-5} \text{ Hz}^{-1/2}$.

To check that the structure of fig. 5 was intrinsic to the mirror itself we repeated the measurements for various initial phases ϑ_0 . Moreover similar measurements performed on

the clean backsurface of the mirror itself gave values of ellipticity compatible with zero within the experimental error showing that the anisotropy of fig. 5 is intrinsic to the mirror layers.

Table 2

Values of ψ_0 and ϑ_0 found in different points of the mirror whose coordinates are x,y

x(cm)	y(cm)	$\psi_0 10^4$	$\vartheta_0(\text{degree})$
-2.0	2.0	3.10	-13
-1.0	2.0	2.52	-19
0.0	2.0	2.20	-19
1.0	2.0	2.01	-21
2.0	2.0	1.58	-24
-2.0	1.0	2.92	-10
-1.0	1.0	2.45	-11
0.0	1.0	2.24	-12
1.0	1.0	1.90	-13
2.0	1.0	1.66	-17
-2.0	0.0	2.65	-3
-1.0	0.0	2.37	-4
0.0	0.0	2.09	-6
1.0	0.0	1.76	-5
2.0	0.0	1.40	-5
-2.0	-1.0	2.76	2
-1.0	-1.0	2.32	3
0.0	-1.0	2.11	-2
1.0	-1.0	1.61	1
2.0	-1.0	1.41	5
-2.0	-2.0	2.86	8
-1.0	-2.0	2.64	5
0.0	-2.0	2.16	15
1.0	-2.0	1.88	11
2.0	-2.0	1.50	9

Since we measured the ratio W_{2v} / W_0 we can set a limit on any anisotropy effect ϵ that causes variations in the reflectivity of the mirror as, for example, linear dichroism.

$$\epsilon < 5 \cdot 10^{-4}$$

As far as we know the surface behaviour shown in table 2 and fig. 5 has never been previously reported. For this peculiar anisotropy we have no explanation.

5. Acknowledgements.

It is a pleasure to acknowledge the strong support of all members of PVLAS collaboration. We thank, also, F.Benedetti, M.Ferluga and G.Gregori for their technical help.

6. References and notes

- [1] Y.Semertzidis et al., Phys. Rev. Lett. **64** 2988 (1990);
R. Cameron et al., J. Opt. Soc. Am. **B3** 520 (1991);
R. Cameron et al., Phys. Lett. **A157** 125 (1991).
- [2] D. Herriot et al., Appl. Opt. **3** 523 (1954);
D. Herriot, H. Schulte, Appl. Opt. **4** 883 (1965).
- [3] S.L.Adler, Ann. Phys. **87** 559 (1971);
E. Iacopini, E. Zavattini, Phys. Lett. **B85** 151 (1979).
- [4] PVLAS INFN Proposal, September 1992.
- [5] M.A. Bouchiat, L. Pottier, Appl. Phys. **B29** 43 (1982);
S. Carusotto et al., Appl. Phys. **B48** 231 (1989).
- [6] L. Dabrowski et al. "Polarization rotation in multipass optical cavity", international conference "from Galileo's occhialino to optoelectronics : frontiers of optical systems and materials", 9-12/6/1992 Padova, Italy;
- [7] S.L. Gilbert, C.E. Wieman, Phys. Rev. **A34** 792 (1986).
- [8] E.Hecht, A.Zajac, "Optics", Addison-Wesley (Reading, Mass. 1987);
- [9] M.Abramowitz, I.A. Stegun, "Handbook of mathematical functions", Dover, N.Y. (1964);
- [10] The mirror was ground by Optical Prototypes Inc., Rochester, N.Y. and was coated by the Laboratory of Laser Energetic of the University of Rochester.